An experimental investigation into a dual taper acoustic black hole termination

K. Hook,[1] **J. Cheer,**[1, a)] **and A. Karlos**[2]

[1)] *Institute of Sound and Vibration Research, University of Southampton, Highfield, Southampton, SO17 1BJ, UK*

[2)] *Department of Robotics and Mechatronics, AGH University of Science and Technology, Al. A. Mickiewicza 30, Krakow, 30-059, Poland*

K.Hook@soton.ac.uk,

J.Cheer@soton.ac.uk,

angelis.karlos@agh.edu.pl

(Dated: 11 August 2022)

Abstract: Acoustic Black Holes (ABHs) can provide effective damping of the reflected wave component when used to terminate a beam. The behaviour of an ABH is characterised by its local modes, which produce narrow frequency bands of high absorption. To enhance the performance of ABH terminations, a multi-taper ABH has previously been proposed and analytical results demonstrate that the use of two or more tapers produces a compound effect on the reflection coefficient, resulting in more bands of low reflection. This paper extends this work and presents an experimental realisation of a multi-taper ABH confirming the previous analytical results.

1. Introduction

The Acoustic Black Hole (ABH) effect is a phenomenon that occurs when propagating waves travel through a structure with a smoothly decreasing thickness profile, which results in a decreasing wave speed. In a practical structure, an ABH can be realised as a power law taper with a small amount of damping applied to the taper to significantly attenuate incident waves. It has previously been shown that the reflection coefficient of an ABH termination is dependent on the local modes of the taper[1–4], which when excited provide critical coupling[2] between the ABH and the host beam and also provide significant absorption of the incident wave due to the large displacement of the taper and decreased wave speed in the taper. As frequency increases, the modal density and overlap increases[3,5] and a lower reflection coefficient is generally achieved. At lower frequencies, however, the bands of low reflection are narrow and ABHs are more suited to narrowband or tonal vibration control problems. The spacing of the bands of low reflection is physically limited by the design of the taper and to achieve significant wave attenuation over a number of closely spaced low frequency bands would require an impractically long taper.

Recently, a multi-taper ABH has been proposed by Karlos *et al.*[6] which addresses the narrowband performance limitations of an ABH termination by introducing multiple tapers. This design approach has parallels to the idea of subordinate oscillators, in which multiple oscillators applied to a structure are variously tuned to improve control[7], but in the case considered here we focus on using multiple ABH tapers, which operate via a different physical mechanism to achieve vibration attenuation. The proposed multi-taper termination

[a] Author to whom correspondence should be addressed.

exhibits a compound behaviour dictated by each of the individual taper geometries and thus introduces more bands of low reflection compared to a single taper design. This paper extends the previous theoretical work on the multi-taper ABH by presenting an experimental investigation into a multi-taper ABH. The paper is organised as follows: firstly, a finite element (FE) model is introduced in Section 2, which has been used to investigate the design of a dual taper ABH; an experimental setup is then presented in Section 3, which has been used to validate the model; finally, the conclusions of this investigation are presented in Section 4.

2. Finite element model

This section contains a description of the FE model that has been used to investigate two single taper terminations and one dual taper termination. The reflection coefficient has been calculated for each termination and there is a discussion of the findings.

2.1 Model description

The FE model used in this investigation has been created in COMSOL Multiphysics using the 3D solid mechanics module. A diagram of the model is shown in Fig. 1 and the dimensions of the model are shown in Table 1. A force of 1 N has been applied to the flat termination

Table 1. The dimensions of the FE model.

Parameter	l_{beam}	l_1	l_2	h_{beam}	b_b	b_s	$h_{tip\ 1}$	$h_{tip\ 2}$	Δ
Value	300 mm	70 mm	100 mm	10 mm	40 mm	1 mm	0.5 mm	0.7 mm	20 mm

of the beam perpendicular to the length of the beam. The dual ABH termination consists

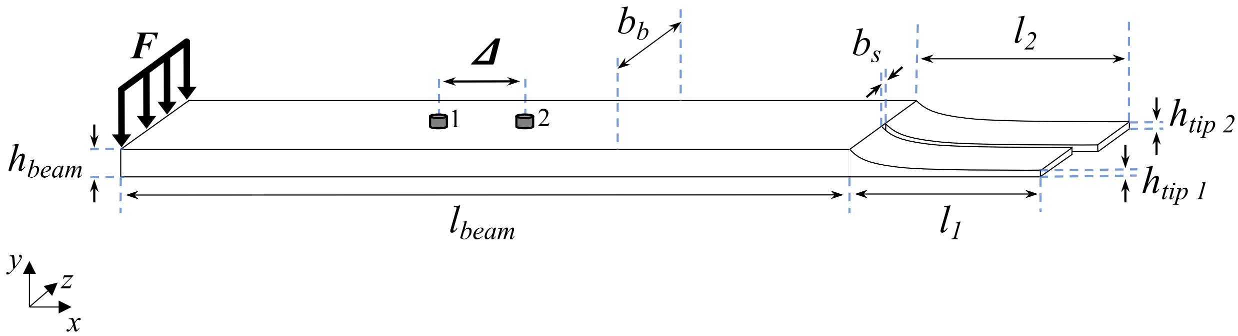

Fig. 1. A diagram showing the dual taper ABH termination.

of a 100 mm taper and a 70 mm taper, separated by 1 mm. Each termination was therefore 19.5 mm wide. The terminations have both been defined using the power law profile

$$h(x) = (h_{beam} - h_{tip\ n}) \left(1 - \frac{x}{l_n}\right)^4 + h_{tip\ n}, \quad (1)$$

where n is used to refer to the parameters of a specific taper and the junction between the constant thickness beam section and the terminating tapers is set at $x = 0$. The beam and tapering terminations have been defined as aluminium, with a density of 2700 kgm^{-3} and a Young's modulus of 70 GPa. The damping layer applied to the terminations has been defined as Henley's yellow compound[8], which has previously been applied to conventional single taper ABH beams and characterised to have a largely frequency independent loss factor of 0.2 across the frequency range considered in this study[3]. A total of 6 g of Henley's yellow compound has been applied to the termination, with the treatment being applied to each taper in a ratio based on the surface areas of the tapers (approx 3.5 g on the 100 mm taper and 2.5 g on the 70 mm taper). In addition to the dual taper ABH termination, two beams with single taper terminations have been modelled in order to benchmark the performance of the dual taper design. One of the single taper configurations has a 100 mm taper and the other has a 70 mm taper, with the full 6 g of Henley's compound applied to each taper. The amount of damping material, therefore, has been kept constant for the three different termination designs, although this means that the total mass of each termination differs due to the differences in the taper geometries. Specifically, the mass of the dual taper is 19% lower than the single 100 mm taper termination and the mass of the single 70 mm taper is 32% lower than the 100 mm taper termination. The single taper configuration models will be used to help demonstrate the combined effect present when using a dual taper. The models have been meshed with triangular elements and a convergence study has been carried out at the upper frequency of interest here, which is 10 kHz. This convergence study demonstrated that the model output converged by 6 elements per wavelength and, therefore, this resolution has been used throughout the following study.

To evaluate the performance of the various beam termination configurations, the response of the beam in both the simulations and the experiments presented in the following section has been evaluated in terms of the reflection coefficient. This can be evaluated via a wave decomposition method, which uses two physical or simulated accelerometers positioned on the constant thickness section of the beam, as shown in Fig. 1. The signals measured from these accelerometers can then be used to estimate the reflection coefficient via a wave decomposition method, which has previously been described in detail for application to ABH performance evaluations[3,9]. Using this method, the complex amplitudes of the incident and reflected wave components can be expressed in terms of the complex acceleration amplitudes at a frequency ω as

$$\begin{bmatrix} \phi^{+}(\omega) \\ \\ \phi^{-}(\omega) \end{bmatrix} = -\frac{1}{\omega^2\left(\mathrm{e}^{\mathrm{i}k\varDelta} - \mathrm{e}^{-\mathrm{i}k\varDelta}\right)} \begin{bmatrix} \mathrm{e}^{\mathrm{i}k(\omega)\frac{\varDelta}{2}} & -\mathrm{e}^{-\mathrm{i}k(\omega)\frac{\varDelta}{2}} \\ \\ -\mathrm{e}^{-\mathrm{i}k(\omega)\frac{\varDelta}{2}} & \mathrm{e}^{\mathrm{i}k(\omega)\frac{\varDelta}{2}} \end{bmatrix} \begin{bmatrix} a_1(\omega) \\ \\ a_2(\omega) \end{bmatrix}, \tag{2}$$

where k is the flexural wavenumber, $\varDelta$ is the sensor separation, ϕ^{+} is the incident wave amplitude midway between the sensors, ϕ^{-} is the reflected wave amplitude midway between the sensors and a_1 and a_2 are the accelerations measured or evaluated at the accelerometer positions.

2.2 Finite Element Results

The models described in Section 2.1 have been run over a frequency range of 100 Hz – 10 kHz and, using Eq. (2), the reflection coefficient has been calculated for two single taper ABH terminations and a dual taper termination combining the two single taper terminations. In addition, the local ABH mode shapes have been extracted from the FE model and are presented with respect to the bands of low reflection. The reflection coefficient results are shown in Fig. 2 and the mode shapes are presented in Figure 3. From the reflection coefficient results presented in Fig. 2, it can be seen that the reflection coefficient of the 70 mm taper has bands of low reflection at 355 Hz, 1.55 kHz, 3.63 kHz and 6.46 kHz. These bands of low reflection are caused by local flexural modes along the length of the taper, which are shown in Figure 3. The reflection coefficient of the 100 mm taper has bands of low reflection at 191 Hz, 832 Hz, 1.95 kHz, 3.47 kHz, 5.37 kHz and 7.76 kHz. Again, these bands of low reflection are caused by the local modes of the taper and the corresponding mode shapes are shown in Figure 3. In the case of the dual taper, it can be seen that a higher number of bands of low reflection are present and occur at 234 Hz, 371 Hz, 1.11 kHz, 1.59

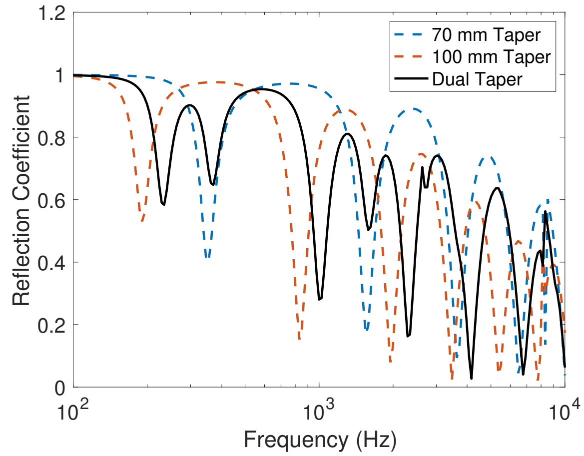

Fig. 2. The reflection coefficient of two individual ABHs and the combined dual taper ABH. The local taper mode shapes corresponding to the bands of low reflection are shown in Figure 3.

Fig. 3. The mode shapes and frequency for each taper configuration.

70 mm Taper	100 mm Taper	Dual Taper
	 191 Hz	 234 Hz
 355 Hz		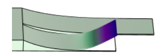 371 Hz
	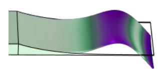 832 Hz	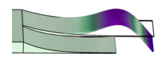 1.11 kHz
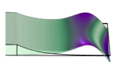 1.55 kHz		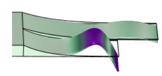 1.59 kHz
	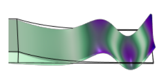 1.95 kHz	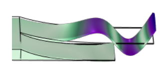 2.30 kHz
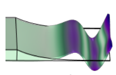 3.63 kHz	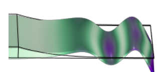 3.47 kHz	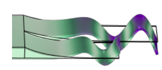 4.17 kHz
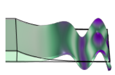 6.46 Hz	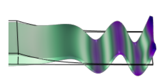 5.37 kHz	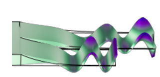 6.76 Hz
	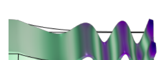 7.76 kHz	

kHz, 2.30 kHz, 4.17 kHz and 6.76 kHz. The local modes of the taper that correspond to the bands of low reflection have been presented in Figure 3. From these results it can be seen that the first five modes of the dual taper configuration correspond to the first two modes of the 70 mm single taper configuration and the first three modes of the 100 mm single taper configuration, albeit with a shift in their resonance frequencies. The sixth and seventh modes of the dual taper configuration correspond to a combination of one mode from each of the single taper configurations, indicating stronger coupling between the two tapers, and again the resonance frequencies are shifted in comparison to the single taper arrangements. The shift in the local taper resonance frequencies can be attributed to a number of factors such as the stiffness change from reducing the width of the taper, the change in the distribution of the damping material applied to the tapers, and the coupling between the two tapers.

In order to compare the different taper configurations, the percentage of the total bandwidth where at least half of the energy is absorbed, $(1-|R|^2) > 0.5$, has been calculated for each termination. The 70 mm taper was effective over 65.9 % of the total bandwidth, the 100 mm taper was effective over 80.8 % of the total bandwidth and the dual taper was effective over 82.2 % of the total bandwidth. Although the bandwidth over which at least half of the energy is absorbed is not significantly increased between the single 100 mm taper and the dual taper configuration, it is important to reiterate that the mass of the dual taper termination is 19 % lower than the mass of the single 100 mm termination, thus demonstrating one potential benefit provided by the multiple taper design. Another potential benefit of the dual taper design is provided by the compound effect, which means that the dual taper termination features more bands of low reflection than either of the single terminations. Although the bands of low reflection are generally less significant in the dual taper configuration, particularly for the dual taper modes corresponding to the shorter taper, the increased number of bands may provide improved design freedom for vibration control applications with multiple narrow band components. As previously demonstrated by Karlos *et al.*[6], the performance of a dual taper termination is highly dependent on the physical parameters of each taper and on the damping and so care must be taken when designing a termination so that the performance gains can be maximised by exploiting the individual behaviour and coupling between the tapers.

3. Experimental investigation

This section presents an experimental investigation, which has been used to validate the model and the dual taper effects previously reported in[6] based on results from analytical models. In the following sections, the experimental setup and methodology is initially described and then the measured reflection coefficient is compared to the modelled results.

3.1 Experimental setup

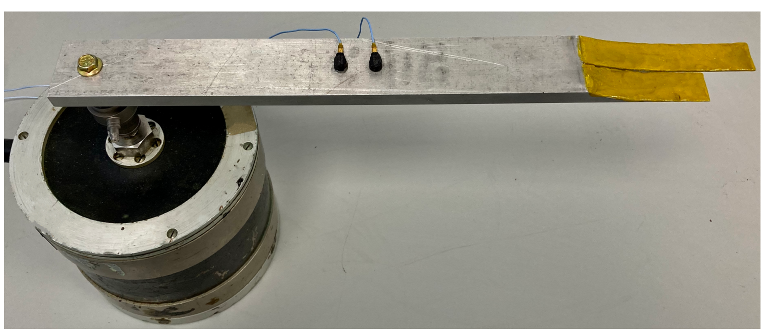

Fig. 4. A Photo showing the experimental setup used to measure the reflection coefficient of the dual ABH termination

A photo of the experimental setup for the dual taper configuration is presented in Fig. 4. The yellow damping material applied to the tapers is Henley's yellow compound. The beam has been mounted onto a large shaker which has been driven with white noise using a sampling frequency of 20 kHz. Low pass filters with a cut-off frequency of 10 kHz have been used for signal anti-aliasing and reconstruction. Two accelerometers have been used to measure the acceleration in the beam section and the frequency responses of each measurement have been calculated using the H1-estimator. Using these frequency responses, the reflection coefficient of the dual taper ABH termination has been calculated using the wave decomposition method outlined in Section 2.1.

3.2 Results

The reflection coefficient calculated using the FE model and the experimentally measured reflection coefficient are presented for the dual termination ABH in Fig. 5. From these

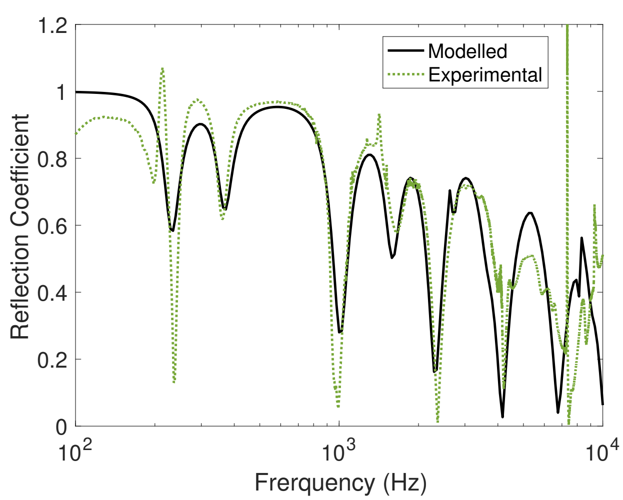

Fig. 5. The reflection coefficient of the dual taper ABH calculated using the FE model and measured experimentally.

results, it can be seen that the experimental reflection coefficient matches the modelled results reasonably well and the compound effect of the two tapers can be seen clearly. The experimental results show slightly lower minima in some of the bands of low reflection, which could be due to the slight differences compared to the modelled damping applied to each of the tapers, and therefore the coupling between the beam and the termination[2]. There is also some variation between the modelled and experimental results below approximately 300 Hz, which can be related to the low frequency limit of the wave decomposition method as described in[3]. Finally, the differences between the modelled and measured results are more significant at frequencies above around 6 kHz and this may be related to frequency dependent behaviour of the damping material in reality, as well as the fact that the mass distribution of the damping material in practice is not perfectly uniform.

4. Conclusions

This express letter has presented a focussed investigation into the experimental realisation of a dual taper ABH termination. It has been shown using an FE model that the dual taper termination exhibits a compound behaviour, featuring local taper modes related to both of the individual tapers. The behaviour of the dual taper ABH termination has then been validated experimentally for the first time. These results have shown that multi-taper ABH terminations introduce additional bands of low reflection and could thus be used to tackle vibration problems when the standard spacing of the bands of low reflection for a single termination are too wide. For the combination of tapers used in this investigation, the effective absorption bandwidth for the dual taper configuration is comparable to that achieved by a single taper termination with the longer taper length, but the dual taper arrangement provides a 19 % reduction in the mass of the termination. By varying the lengths of the dual tapers and the damping it is possible to tune the response of the termination[6] and additional tapers could be added to introduce further bands of low reflection.

Acknowledgment

This work was supported by the Intelligent Structures for Low Noise Environments (ISLNE) EPSRC Prosperity Partnership (EP/S03661X/1). Angelis Karlos acknowledges support from the National Science Centre in Poland through Grant No. 2018/31/B/ST8/00753.

References and links

[1] Ji, H., Han, B., Cheng, L., Inman, D.J. and Qiu, J. (**2002**). "Frequency attenuation band with low vibration transmission in a finite-size plate strip embedded with 2D acoustic black holes," Mechanical Systems and Signal Processing, **163**, 1–14.

[2] Leng, H., Romero-García, V., Pelat, A., Picó, R., Groby, J.P. and Gautier, F. (**2020**). "Interpretation of the Acoustic Black Hole effect based on the concept of critical coupling," Journal of Sound and Vibration, **471**, 1–10.

[3] Hook, K., Cheer, J., and Daley, S. (**2019**). "A Parametric Study of an Acoustic Black Hole on a Beam," The Journal of the Acoustical Society of America **145**(6), 3488–3498.

[4] Pelat, A., Gautier, F., Conlon, S.C. and Semperlotti, F. (**2020**). "The acoustic black hole: A review of theory and applications," Journal of Sound and Vibration, **476**, 1–24.

[5] Denis, V., Pelat, A., Gautier, F. and Elie, B. (**2014**). "Modal overlap factor of a beam with an ABH termination," Journal of Sound and Vibration **333**(12), 2475–2488.

[6] Karlos, A., Hook, K. and Cheer, J. (**2022**). “Enhanced absorption with multiple quadratically tapered elastic wedges of different lengths terminating a uniform beam,” Journal of Sound and Vibration **531**, 1–13.

[7] Vignola, J. F. and Judge, J. (**2009**) “Shaping of a system’s frequency response using an array of subordinate oscillators,” The Journal of the Acoustical Society of America, **126**, 129–139.

[8] Henley, W.T. “Yellow plastic compound,” https://www.wt-henley.com/cable_accessories-green_and_yellow_plastic_compound.html, 2021 (Last Accessed: 06/02/2021).

[9] Cheer, J., Hook, K. and Daley, S. (**2021**) “Active feedforward control of flexural waves in an Acoustic Black Hole terminated beam,” Smart Materials and Structures, **30**(3), 1–14.